Annals of the BMVA Vol. 2009, No. 7, pp 1–9 (2009)

Identification of atrophy patterns in Alzheimer's disease based on SVM feature selection and anatomical parcellation

L. Mesrob[1,2,3], B. Magnin[2,3,4], O. Colliot[3,5], M. Sarazin[2,3,6], V. Hahn-Barma[7], B. Dubois[2,3,6], P. Gallinari[1], S. Lehéricy[2,3,8,9], S. Kinkingnéhun[2,3,10] and H. Benali[3,4]

[1]LIP6, UPMC Univ Paris 06, Paris, France
[2]UMR-S 610, Inserm, Paris, France
[3]IFR 49, Gif-sur-Yvette, France
[4]UMR-S 678, Inserm, Paris, France
[5]UPR 640 LENA, CNRS, Paris, France
[6]Department of Neurology, Pitié-Salpêtrière Hospital, Paris, France
[7]Research and Resource Memory Centre, Pitié-Salpêtrière Hospital, Paris, France
[8]Department of Neuroradiology, Pitié-Salpêtrière Hospital, Paris, France
[9]Center for NeuroImaging Research – CENIR, Paris, France
[10]e(ye)BRAIN, Ivry-sur-Seine, France

<lmesrob@yahoo.fr>

Abstract

In this paper, we propose a fully automated method to individually classify patients with Alzheimer's disease (AD) and elderly control subjects based on anatomical magnetic resonance imaging (MRI). Our approach relies on the identification of gray matter (GM) atrophy patterns using whole-brain parcellation into anatomical regions and the extraction of GM characteristics in these regions. Discriminative features are identified using different feature selection (FS) methods and used in a Support Vector Machine (SVM) for individual classification. We compare two different types of parcellations corresponding to two different levels of anatomical details. We validate our approach with two distinct groups of subjects: an initial cohort of 16 AD patients and 15 elderly controls and a second cohort of 17 AD patients and 13 controls. We used the first cohort for training and region selection and the second cohort for testing and obtained high classification accuracy (90%).

1 Introduction

Due to aging of the population, Alzheimer's disease (AD) is increasingly becoming a crucial public health issue [1]. Early detection and diagnosis of AD is an important task which would enable more effective treatment of patients with currently available medication

such as cholinesterase inhibitors [2]. AD is characterized by progressive gray matter (GM) loss which occurs presymptomatically in some neuroanatomical structures [3]. Thus, magnetic resonance imaging (MRI) measurements, primarily in the GM, could be sensitive markers of the disease and assist early diagnosis.

MRI studies in AD have demonstrated that volumetry of medial temporal lobe (MTL) anatomical structures, such as the hippocampus, the amygdala and the entorhinal cortex can be useful in the diagnosis of AD [4-7]. However, in AD, even though atrophy starts in the MTL, it is not confined to these regions and patients present with a distributed spatial pattern of atrophy. Moreover, MTL atrophy is not specific of AD and is also present in other forms of dementia. There has thus recently been a growing interest for high-dimensional classification methods that can combine information from anatomical regions distributed over the whole brain to discriminate between individual subjects [8-10].

In this paper, we propose a method to automatically discriminate between patients with AD and elderly control subjects based on Support Vector Machine (SVM) [11] classification from whole brain anatomical MRI. Our approach is based on a parcellation of the MRI into different regions in which tissue characteristics are estimated [12]. We compare two different types of parcellations corresponding to two different levels of details. We introduce a feature selection (FS) approach whose aim is to identify regions contributing to the pattern of atrophy of AD. We perform and compare two different FS methods: an univariate and a multivariate approach. Moreover, we introduce a bootstrap [13] procedure in order to obtain more robust estimates of the classification results. We validate our approach in two distinct cohorts of subjects composed of AD patients and elderly healthy controls matched for age and gender.

2 Method

Our approach is composed of the following steps. Individual MR images are first parcellated into anatomical regions of interest (ROI) using registration with a labelled template (Section 2.1). In addition to a standard parcellation based on the Automated Anatomical Labeling (AAL) [14], we also propose a refined parcellation which corresponds to a more specific level of anatomical details (Section 2.2). Tissue characteristics of gray matter (GM), white matter (WM) and cerebrospinal fluid (CSF) are then extracted separately in each of these ROIs (Section 2.3). The most discriminative regions are then identified using a univariate and a multivariate FS method (Section 2.4). Individual subjects are finally classified using a non-linear SVM (Section 2.5). Robust estimates of classification results are obtained using a bootstrap approach.

2.1 Brain Parcellation into 90 Regions Using AAL

The first parcellation that we propose relies on the AAL introduced by Tzourio-Mazoyer et al. [14]. MR images were automatically parcellated into 90 anatomical ROI using the spatial normalization module of SPM2 (Statistical Parametric Mapping, University College London, UK). The 90 anatomical regions correspond to all cortical structures included in the AAL atlas except the cerebellum. In the first step, the MRI of each subject was warped to the Montreal Neurological Institute (MNI) standard space applying affine registration followed by 16 iterations of nonlinear deformations (linear combination of cosine transform basis functions). The SPM2 default parameters were used. Then, the inverse transformation was applied to warp the anatomical atlas AAL to the individual's space resulting in the parcellation of the original MRI into 90 regions.

Annals of the BMVA Vol. 2009, No. 7, pp 1–9 (2009)

2.2 Refined Brain Parcellation into 487 Regions

The AAL atlas provides an anatomical driven parcellation. However, certain structures are very large compared to others. Early AD is characterized by local alterations in some sensitive regions such as the hippocampus and medial temporal lobe. These early changes, relatively well identified in group voxel-based analyses, could go undetected when extracting parameters from a too large region. The effect of the local damage is then "diluted" and is not revealed at the scale of the whole region. It is thus of interest to assess whether a refined parcellation would provide increased sensitivity to subtle alterations.

To address this issue, we propose a refinement of the AAL atlas with the two following constraints: 1) the volume of the new regions should not be less than that of the smallest structure in the AAL, namely the amygdala, (250 voxels with voxel size=2x2x2 mm^3) and 2) the presence of the three brain tissues (GM, WM and CSF) should be preserved in the new structures. The first constraint led to the subdivision of 80 from the 90 ROI into 477 smaller regions. Thus, the new atlas contained 487 ROI (Figure 1). The second constraint was necessary to ensure good separation of the Gaussian models, i.e. the correct parameter extraction (see Section 2.3). To that purpose, we aimed at subdividing the regions following the plan that was approximately orthogonal to the cortical surface. Anatomical structures in the anterior and posterior portions of the brain were divided in sub regions following the inferosuperior direction, whereas structures in the superior and lateral portions were parcellated following the anteroposterior direction. This algorithm is an approximation of the theoretical one which should subdivide the regions orthogonally to the cortical surface, in order to be sure to keep voxels from the three tissues in each ROI.

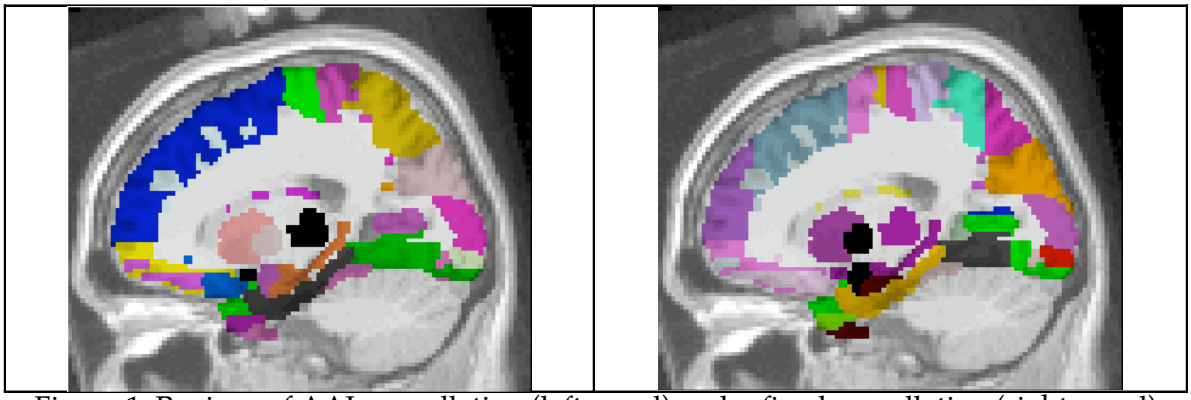

Figure 1: Regions of AAL parcellation (left panel) and refined parcellation (right panel) illustrated on the same sagittal slice (+19.5 mm) of the MNI structural template.

2.3 Parameter Extraction

Local tissue parameter extraction was performed in each ROI using a Gaussian Mixture Model (GMM) where Gaussians describe the voxel intensity distribution of the three brain tissues: GM, WM and CSF [12]. The first Gaussian corresponds to the CSF, the second to the GM and the third to the WM. This Gaussian mixture can be represented as:

$$\alpha_1 * N(\mu_1, \sigma_1^2) + \alpha_2 * N(\mu_2, \sigma_2^2) + \alpha_3 * N(\mu_3, \sigma_3^2), \text{ where } \alpha_1 + \alpha_2 + \alpha_3 = 1$$

where α_i is the weight coefficient, μ_i the mean, and σ_i the standard deviation of each Gaussian.

These parameters were estimated with the Expectation Maximization (EM) algorithm [15]. The weighted ratio $\alpha_2 * \mu_2 / \sigma_2$ between the mean and the standard deviation of the GM

Gaussian was used for the subjects' classification. The feature vector for each subject was thus constituted by the weighted ratio for each of the 90 regions.

2.4 Feature Selection

The aim of this step is to identify the most relevant features (or parameters) for the classification. We performed a univariate FS approach. The discriminating power of the feature parameter in each ROI was assessed by using a two-sample *t*-test. The probability distribution was generated by using a bootstrap method, working with the null hypothesis H_0 that there is no difference between the two groups of subjects. To obtain a good estimation of the *p* value of the *t*-test, we performed the method with a large number of resamplings (5000). According to the *p* value, we determined the significance of the *t*-test for each ROI. Thus, the most significantly different ROIs ($p<10^{-2}$) were selected as being the most relevant for the discrimination.

We also performed a multivariate FS approach based on the SVM-Recursive Feature Elimination (SVM-RFE) [16] algorithm. The algorithm estimates at each step the features' weights (using linear SVM) and rejects the features with the least weights keeping in the end the most relevant features. In order to determine the optimal number of features to select, we applied recursively the SVM-RFE eliminating at each iteration only one feature and calculating the classification accuracy of the selected ones. To obtain a more robust FS, we embedded a bootstrap with 500 resamplings in this procedure. To this purpose, we drew without replacement approximately 75% of each group to obtain a training set. The remaining 25% were used as a test set. The procedure was repeated 500 times. We thus obtained the correct classification rate for the 500 drawings. Thus, for each level corresponding to the number of selected features, the eliminated feature was the most frequently chosen one within the different resamplings and the cross-validation (CV) error was estimated as the mean of the 500 samples' CV errors. The level with the least CV error gave the optimal number of features and the set of the selected features.

In our application, the selected features correspond to MRI measurements in anatomical structures. The parameters extraction being based on the GM distribution in the ROI, we hypothesize that the FS step will identify brain structures altered by the neurodegenerative pathology.

2.5 Classification Method

Subjects' classification was performed using nonlinear SVM [11] with radial basis function (RBF) kernel. To obtain robust estimates of the classification accuracy, a bootstrap with 5000 resamplings was added in the learning and cross-validation steps. Bootstrap is a generalization of the leave one out (LOO) method. The large number of samples insures that every subject's data have participated in the cross-validation step. Here again, we drew without replacement approximately 75% of each group to obtain a training set and the remaining 25% were used as a test set. Accuracy was evaluated for every subset of data and global accuracy was evaluated as the mean of the 5000 resamplings.

The optimal values of the two SVM parameters - γ (width of the RBF) and C (error/trade-off parameter), were determined using a grid search. Using the bootstrap procedure for training and test selection, we performed classifications for the MRI dataset with (γ,C) varying along a grid, with a search range of $[2^{-5}, 2^{10}]$ for C and $[2^{-10}, 2^{5}]$ for γ. The value of (γ,C) that gave the best classification accuracy was then used to build the classifier.

Annals of the BMVA Vol. 2009, No. 7, pp 1–9 (2009)

3 Experiments and Results

3.1 Validation Data

The validation of the algorithm was performed using two different cohorts which were parts of two distinct studies. AD patients fulfill the National Institute of Neurological and Communication Disorders and Stroke/AD and Related Disorders Association criteria for probable AD [17]. The initial cohort (Cohort 1) included 15 AD patients (mean age±standard deviation (SD)=70.2±6, mini-mental score (MMS)=23.6±2.5, five males, ten females) and 16 elderly healthy controls (age=71.0±4, MMS=29.0±1, six males, ten females). A second cohort (Cohort 2) included 17 AD patients (age=74.5±5, MMS=23.6±2, five males, twelve females) and 13 controls (age=70.0±7, MMS=28.3±1.4, four males, nine females). Patients were recruited at the Research and Resource Memory Center of the Pitié-Salpêtrière hospital. The local ethics committee approved the study and written informed consent was obtained from all participants. In each subject, a T1-weighted volume MRI scan was acquired using the spoiled gradient echo sequence (SPGR) (TR/TE/flip angle: 23ms/5ms/35°, 256×256 matrix; voxel size=0.859x0.859x1.5mm^3) on a 1.5T scanner (General Electric, Milwaukee, WI, USA).

3.2 Cross-Validation Results with Initial Cohort

The univariate FS method was performed with the original 90 ROI atlas and identified 18 ROIs with p value less than 10^{-2}. The most significant ROIs included regions classically affected in AD, such as the hippocampus or the parahippocampal gyrus.

Univariate ROIs selection ROI's name in AAL atlas	Multivariate ROIs selection ROI's name in AAL atlas
ParaHippocampal_R	**Frontal_Sup_Orb_L**
Frontal_Sup_Orb_L	**Frontal_Mid_R**
Calcarine_L	Supp_Motor_Area_L
Hippocampus_L	**Hippocampus_L**
Frontal_Mid_R	**ParaHippocampal_L**
Temporal_Sup_R	**ParaHippocampal_R**
Cingulum_Mid_R	**Calcarine_L**
ParaHippocampal_L	Fusiform_R
Rectus_L	Putamen_R
Frontal_Inf_Orb_R	Temporal_Pole_Sup_L
Temporal_Pole_Mid_R	Temporal_Pole_Sup_R
Frontal_Mid_Orb_R	Temporal_Inf_L
Rectus_R	
Frontal_Sup_Orb_R	
Occipital_Inf_R	
Parietal_Inf_R	
Occipital_Inf_R	
Cingulum_Mid_R	

Table 1 : Univariate and multivariate AAL's ROIs selection. In bold the ROIs selected by both algorithms.

The SVM-RFE algorithm identified 12 regions from the original 90 ROI atlas and 43 regions from the refined 487 ROI atlas as being the most relevant for the discrimination. The value of (γ,C) was set to (0.870551, 2.639016). Selected regions included (but not only) the hippocampus, the parahippocampal gyrus, the precuneus, the calcarine, the posterior cingulate gyrus, the inferior and the polar temporal regions (Figure 2). Interestingly, the set of selec-

ted regions with the multivariate approach included some regions that were estimated as non significantly different using the two-sample *T* test (see Table 1).

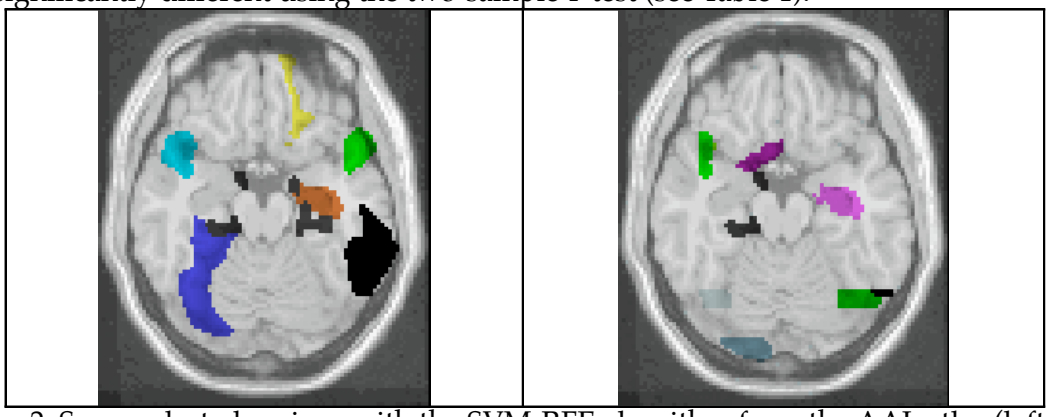

Figure 2: Some selected regions with the SVM-RFE algorithm from the AAL atlas (left panel) and from the refined atlas (right panel) illustrated on the MNI structural template.

The results from the following classification experiments are summarized in Table 2:

- to assess the added value of our local tissue segmentation method, we compared the results obtained with the features extracted from the EM algorithm ($\alpha^*\mu/\sigma$ in each region) to those obtained with the mean GM concentration in each region i.e. the mean probability of the voxels to belong to the GM given by the standard tissue segmentation procedure in SPM2;
- we compared the results obtained using the original 90 ROI parcellation to those obtained using the refined 487 ROI parcellation;
- we compared the results obtained using all regions to those obtained using only the regions selected by the univariate or the multivariate FS methods.

MRI measurement	Nb features	Parcellation Type	Specificity (%)	Sensitivity (%)	Accuracy (%)
GM concentration	90 Original	90 ROI	66.1	65.8	66.0
GM $\alpha^*\mu/\sigma$	90 Original	90 ROI	74.3	78.7	76.5
GM $\alpha^*\mu/\sigma$	18 Original univariate	90 ROI	87.0	73.4	80.2
GM $\alpha^*\mu/\sigma$	12 Original multivariate	90 ROI	98.8	99.0	98.9
GM $\alpha^*\mu/\sigma$	487 Refined	487 ROI	66.0	53.6	59.8
GM $\alpha^*\mu/\sigma$	43 Refined	487 ROI	99.8	99.9	99.9

Table 2: Classification results obtained for Cohort 1 with different MRI measurements, different number of features and different types of parcellations.

3.3 Evaluation on Data from Another Cohort

In Cohort 1, the SVM-RFE algorithm allowed achieving very good classification results (close to 100%). However, it is unclear whether the selected regions are representative of the atrophy distribution in AD or if they are specific to this particular group of subjects. In other words, it is necessary to assess the generalization ability of the FS step. To that purpose, we used the regions selected from Cohort 1 to discriminate subjects from Cohort 2. Classification accuracy was assessed by performing cross validation with Cohort 2 and inter-cohort validation, where Cohort 1 was used as a training dataset and Cohort 2 as a test dataset. This was done with both the 12 regions selected from the original 90 ROI parcellation and the 43 regions selected from the refined 487 ROI parcellation. The results are presented in Table 3.

MRI measurement	Nb features	Parcellation type	Training dataset	Specificity (%)	Sensitivity (%)	Accuracy (%)

GM α*μ /σ	12	90 ROI	Cohort 1	96.0	84.3	90.2
GM α*μ /σ	12	90 ROI	Cohort 2	88.6	93.7	91.1
GM α*μ /σ	43	487 ROI	Cohort 1	62.3	85.9	74.1
GM α*μ /σ	43	487 ROI	Cohort 2	80.9	84.0	82.5

Table 3: Classification results obtained for Cohort 2 when performing FS on Cohort 1 and SVM training with different datasets.

4 Discussion and Conclusion

In this paper, we proposed a method to discriminate between patients with AD and elderly controls based on SVM classification, whole-brain anatomical parcellation and different FS approaches.

In order to derive an index of local brain atrophy, we estimated tissue characteristics in each of the parcelled regions. This index provided a good discrimination between patients and controls, indicating that it is a sensitive marker of early AD. In particular, it proved superior to a standard measurement of GM concentration (76.5% instead of 66%).

We introduced two FS approaches: a univariate approach based on the two-sample *t* test and a multivariate approach based on the SVM-RFE algorithm. Though the selection was data driven and not based on prior knowledge, both methods selected regions known to be early altered in the degenerative disease such as the hippocampus, the parahippocampal gyrus, the precuneus and the temporal lobes. The FS provided increased classification accuracy on Cohort 1, slightly with the univariate approach (80.2% instead of 76.5%) and more importantly with the multivariate one (98.9% instead of 76.5%). Thus, the best classification results were obtained with the multivariate FS method. Most of the regions selected with the SVM-RFE algorithm were significantly different ($p<10^{-2}$) between AD patients and controls but some were not. Thus, identifying a discriminating subset of features seems to be more robust and relevant for the classification than combining the most discriminating features identified with the univariate FS approach. The fact that some regions selected with the SVM-RFE algorithm were not significantly different between AD and control emphasized the importance of the pattern of lesion in the discrimination of the two groups. It should be noted that the added value of the FS step might be accentuated by the fact that the subjects groups were relatively small. Importantly, results showed a good generalization ability of this FS step as a high classification accuracy was maintained when using a different cohort for validation (>90%) while using the regions selected from the initial one. Moreover, good classification accuracy was achieved in both inter-cohort and cross validations. This suggests that the selected regions are representative of the pattern of atrophy in AD.

We proposed a refined brain parcellation whose aim was to divide the large regions of the AAL atlas into smaller sub regions whilst preserving the presence of the three brain tissues. Our purpose was to assess whether a refined parcellation would allow detecting more subtle alterations of the gray matter. While this refined parcellation provided good classification results on Cohort 1 (when combined with the FS step), this was not the case for the inter-cohort validation where the classification accuracy dropped to 74%. This seems to indicate that the selected regions of the refined atlas do not have good generalization ability and are rather specific of the cohort which has been used for selection.

It can be noticed that the refinement process lead to a drop of the accuracy when the ROIs were not selected (see Table 2). This can be explained by the size of the NAAL's ROIs. Some ROIs may be too small regarding the pathology. Since the pathology does not progress linearly in each ROI, some ROIs may be randomly affected. There might also be some problems due to the sub-division process which does not leave tissues in each of the

ROI, leading to a bad parameter extraction and thus to low accuracy. But after refinement, a selection of the best subdivided and/or systematically involved ROIs is done which improves the classification.

We chose to keep two separated cohorts in order to provide a completely unbiased evaluation of the classification. However, this resulted in smaller validation groups. Future validations on larger groups such as the ADNI data-set (www.loni.ucla.edu/ADNI) are required to confirm the results of the present study. Another interesting investigation would be the prognosis power of AD given cases of mild cognitive impairment (MCI).

Recently, several groups have used SVM classification to discriminate between patients with AD and elderly controls based on whole-brain anatomical MRI. Klöppel et al. [8] achieved 92%-95% accuracy on AD patients with average MMS of about 16 but the result dropped to 81% when considering more early patients (mean MMS equal to 23.5). Vemuri et al. [9] obtained about 89% accuracy when combining MR data with demographical and genetic information (median MMS between 20 and 22). Fan et al. [10] achieved 94% accuracy between AD patients and controls (mean MMS equal to 23). Our best inter-cohort validation results reached 90.2% accuracy. Our method differentiated from these studies on application of SVM on fMRI images [18] using bootstrap procedure in order to obtain more robust estimates of the classification. The features themselves are different from other studies, since they are not sets of voxels or a mean of a signal but characteristics of the grey matter distribution.

In conclusion, we have introduced a method to automatically discriminate between patients with AD and elderly controls. Using separate learning and test datasets, we obtained high classification accuracy. This new approach has potential to become a useful tool to assist in the early diagnosis of AD.

5 References

[1] C.P. Ferri, M. Prince, C. Brayne, H. Brodaty, L. Fratiglioni, M. Ganguli, K. Hall, K. Hasegawa, H. Hendrie, Y. Huang, A. Jorm, C. Mathers, P.R. Menezes, E. Rimmer, et M. Scazufca, "Global prevalence of dementia: a Delphi consensus study," *Lancet*, vol. 366, Déc. 2005, pp. 2112-2117.

[2] B. Dubois, H.H. Feldman, C. Jacova, S.T. DeKosky, P. Barberger-Gateau, J. Cummings, A. Delacourte, D. Galasko, S. Gauthier, G. Jicha, K. Meguro, J. O'Brien, F. Pasquier, P. Robert, M. Rossor, S. Salloway, Y. Stern, P.J. Visser, et P. Scheltens, "Research criteria for the diagnosis of Alzheimer's disease: revising the NINCDS-ADRDA criteria," *The Lancet Neurology*, vol. 6, Aoû. 2007, pp. 734-746.

[3] N.C. Fox, E.K. Warrington, P.A. Freeborough, P. Hartikainen, A.M. Kennedy, J.M. Stevens, et M.N. Rossor, "Presymptomatic hippocampal atrophy in Alzheimer's disease. A longitudinal MRI study," *Brain*, vol. 119, 1996, pp. 2001-2007.

[4] C.R.J. Jack, R.C. Petersen, Y.C. Xu, P.C. O'Brien, G.E. Smith, R.J. Ivnik, B.F. Boeve, S.C. Waring, E.G. Tangalos, et E. Kokmen, "Prediction of AD with MRI-based hippocampal volume in mild cognitive impairment," *Neurology*, vol. 52, 1999, pp. 1397-1403.

[5] B.C. Dickerson, I. Goncharova, M.P. Sullivan, C. Forchetti, R.S. Wilson, D.A. Bennett, L.A. Beckett, et L. deToledo-Morrell, "MRI-derived entorhinal and hippocampal atrophy in incipient and very mild Alzheimer's disease," *Neurobiology of Aging*, vol. 22, Oct. 2001, pp. 747-754.

[6] P.J. Visser, F.R. Verhey, P.A. Hofman, P. Scheltens, et J. Jolles, "Medial temporal lobe atrophy predicts Alzheimer's disease in patients with minor cognitive impairment," *J Neurol Neurosurg Psychiatry*, vol. 72, 2002, pp. 491-7.

[7] A.T. Du, N. Schuff, J.H. Kramer, S. Ganzer, X.P. Zhu, W.J. Jagust, B.L. Miller, B.R. Reed, D. Mungas, K. Yaffe, H.C. Chui, et M.W. Weiner, "Higher atrophy rate of entorhinal cortex than hippocampus in AD," *Neurology*, vol. 62, 2004, pp. 422-7.

[8] S. Klöppel, C.M. Stonnington, C. Chu, B. Draganski, R.I. Scahill, J.D. Rohrer, N.C. Fox, C.R. Jack, J. Ashburner, et R.S.J. Frackowiak, "Automatic classification of MR scans in Alzheimer's disease," *Brain: A Journal of Neurology*, vol. 131, Mar. 2008, pp. 681-689.

[9] P. Vemuri, J.L. Gunter, M.L. Senjem, J.L. Whitwell, K. Kantarci, D.S. Knopman, B.F. Boeve, R.C. Petersen, et C.R. Jack, "Alzheimer's disease diagnosis in individual subjects using structural MR images: validation studies," *NeuroImage*, vol. 39, Fév. 2008, pp. 1186-1197.

[10] Y. Fan, N. Batmanghelich, C.M. Clark, et C. Davatzikos, "Spatial patterns of brain atrophy in MCI patients, identified via high-dimensional pattern classification, predict subsequent cognitive decline," *NeuroImage*, vol. 39, Fév. 2008, pp. 1731-1743.
[11] C. Cortes et V. Vapnik, "Support-Vector Networks," *Machine Learning*, vol. 20, 1995.
[12] B. Magnin, L. Mesrob, S. Kinkingnéhun, M. Pélégrini-Issac, O. Colliot, M. Sarazin, B. Dubois, S. Lehéricy, et H. Benali, "Support vector machine-based classification of Alzheimer's disease from whole-brain anatomical MRI," *Neuroradiology*, vol. 51, Fév. 2009, pp. 73-83.
[13] B. Efron et R. Tibshirani, *An introduction to the bootstrap*, CRC Press, 1993.
[14] N. Tzourio-Mazoyer, B. Landeau, D. Papathanassiou, F. Crivello, O. Etard, N. Delcroix, B. Mazoyer, et M. Joliot, "Automated anatomical labeling of activations in SPM using a macroscopic anatomical parcellation of the MNI MRI single-subject brain," *Neuroimage*, vol. 15, 2002, pp. 273-89.
[15] R.A. Redner et H.F. Walker, "Mixture Densities, Maximum Likelihood and the EM Algorithm," *SIAM Review*, vol. 26, Avr. 1984, pp. 195-239.
[16] I. Guyon, J. Weston, S. Barnhill, et V. Vapnik, "Gene Selection for Cancer Classification using Support Vector Machines," *Machine Learning*, vol. 46, 2002, pp. 389–422.
[17] G. McKhann, D. Drachman, M. Folstein, R. Katzman, D. Price, et E.M. Stadlan, "Clinical diagnosis of Alzheimer's disease: report of the NINCDS-ADRDA Work Group under the auspices of Department of Health and Human Services Task Force on Alzheimer's Disease," *Neurology*, vol. 34, 1984, pp. 939-944.
[18] F. De Martino, G. Valente, N. Staeren, J. Ashburner, R. Goebel, et E. Formisano, "Combining multivariate voxel selection and support vector machines for mapping and classification of fMRI spatial patterns," *NeuroImage*, vol. 43, Oct. 2008, pp. 44-58.